PHYSICAL REVIEW B **83**, 241101(R) (2011)

Polarization-analyzed resonant inelastic x-ray scattering of the orbital excitations in $KCuF_3$

K. Ishii,[1] S. Ishihara,[2,3] Y. Murakami,[1,2,4] K. Ikeuchi,[1,4] K. Kuzushita,[1] T. Inami,[1] K. Ohwada,[1] M. Yoshida,[1] I. Jarrige,[1] N. Tatami,[2] S. Niioka,[2] D. Bizen,[2] Y. Ando,[2] J. Mizuki,[1] S. Maekawa,[3,5] and Y. Endoh[1,6]

[1]*SPring-8, Japan Atomic Energy Agency, Hyogo 679-5148, Japan*

[2]*Department of Physics, Tohoku University, Sendai 980-8578, Japan*

[3]*CREST, Japan Science and Technology Agency (JST), Tokyo 102-0075, Japan*

[4]*Photon Factory / Condensed Matter Research Center, Institute of Materials Structure Science, High Energy Accelerator Research Organization (KEK), Tsukuba 305-0801, Japan*

[5]*Advanced Science Research Center, Japan Atomic Energy Agency, Tokai 319-1195, Japan*

[6]*International Institute for Advanced Studies, Kizu, Kyoto 619-0025, Japan*

(Received 18 May 2011; published 16 June 2011)

We report a Cu *K* edge resonant inelastic x-ray scattering (RIXS) study of the orbital excitations in the orbital-ordered Mott insulator $KCuF_3$. By performing the polarization analysis of the scattered photons, the excitation between the e_g orbitals is successfully distinguished from the excitations from t_{2g} to e_g. The polarization dependence of the respective excitations is interpreted based on a phenomenological consideration of the symmetry of the RIXS process that yields a necessary condition for observing the excitations. Owing to our polarization analysis, we are able to measure the momentum dependence of the orbital excitation corresponding to the orbital degree of freedom over the whole Brillouin zone. The excitation is found to be dispersionless within our experimental resolution.

DOI: 10.1103/PhysRevB.83.241101 PACS number(s): 78.70.Ck, 75.25.Dk

Strongly correlated transition metal compounds attract great interest because of a variety of interesting properties such as high-temperature superconductivity in cuprates and colossal magnetoresistance in manganites.[1] It is widely recognized that the three degrees of freedom of the *d* electron (i.e., charge, spin, and orbital) play a crucial role in the occurrence of these phenomena. Hence spectroscopic investigations to measure the excitations of these degrees of freedom are required to elucidate their underlying interactions. The observation of the excitation of the orbital degree of freedom is yet difficult because intra-atomic *d*-*d* (orbital) excitations are forbidden within the dipole approximation, and accordingly a second-order optical process is required. While the orbital excitation at zero momentum transfer has been observed in $LaMnO_3$ using Raman scattering,[2] an experimental technique with momentum resolution is crucial to the complete understanding of the elementary orbital excitation; the so-called orbiton. In this respect, inelastic x-ray scattering (IXS) is an ideal candidate, especially in the hard x-ray regime where one can explore a wide momentum range. A recent nonresonant IXS study showed that the *d*-*d* excitations can be observed at high momentum transfer,[3] although nonresonant IXS usually suffers from low intensity. This shortcoming can be overcome by using resonant inelastic x-ray scattering (RIXS), where the incident photon energy is tuned near an absorption edge of a constituent element, resulting in a significant resonant enhancement of the electronic excitations.[4,5] RIXS spectra are primarily related to the dynamical charge correlation.[6,7] Furthermore, spin[8–10] and orbital[11,12] excitations have also become accessible with the more recently developed spectrometers and their improved energy resolution.

In general, the RIXS spectrum is a function of energy, momentum, and polarization of both the incident and scattered photons. However, most RIXS studies so far have focused on energy and momentum dependencies, while the polarization, which is an inherent and important characteristic of the photon, was overlooked. The role of the incident photon polarization was investigated in relation with the resonant conditions in a few experimental and theoretical studies[13–17] and selection rules for the incident polarization was discussed in an unpublished work.[18] In contrast, the scattered photon polarization has not been identified at all. Like conventional Raman spectroscopy, polarization in RIXS must be connected to the symmetry of the excitations. Because the symmetry argument is rigorous and independent of the parameters in theoretical models, the polarization can be very useful for the assignment of the excitations in RIXS.

In this Rapid Communication, we report on a polarization analysis of the Cu *K* edge RIXS of the orbitally ordered compound $KCuF_3$ and demonstrate that the observation of the orbital (*d*-*d*) excitations by RIXS depends on the polarization conditions. $KCuF_3$ has long been known to display quantum one-dimensional antiferromagnetic properties along the *c* axis originating from the strong superexchange interaction between the e_g orbitals of Cu^{2+}.[19] While the two e_g orbitals are degenerate under the cubic symmetry, in the real tetragonal structure the degeneracy is lifted, accompanied with the occurrence of strong Jahn-Teller distortions. The e_g orbitals are ordered according to the pattern shown in the inset of Fig. 1, which corresponds to an alternation of the hole orbitals $3d_{y^2-z^2}$ and $3d_{z^2-x^2}$ on adjacent Cu sites. There are two types of orbital excitations in $KCuF_3$: One excitation is a transition of an electron from the t_{2g} orbital to the e_g orbital (t_{2g} excitation) and the other one is between the e_g orbitals (e_g excitation). The latter excitation is unique to the orbital-ordered Mott insulators. By analyzing the scattered photon polarization, these two types of orbital excitations are successfully distinguished based on a phenomenological group-theoretical consideration of RIXS, which enables us to investigate the momentum dependence of each orbital excitation separately over the whole Brillouin

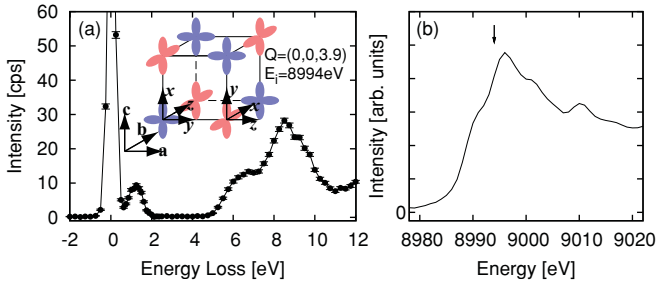

FIG. 1. (Color online) (a) Typical RIXS spectrum of $KCuF_3$. The inset shows a schematic representation of the orbital order of $KCuF_3$ in the hole picture. (b) X-ray absorption spectrum of polycrystalline $KCuF_3$. The incident photon energy for the RIXS measurement is indicated by the arrow.

zone. The excitations are found to be dispersionless within our experimental resolution.

The experiments were carried out at BL11XU at SPring-8. Incident x-rays were monochromatized by a double crystal Si(111) monochromator and a secondary Si(400) channel-cut monochromator. Scattered x-rays were analyzed in energy by spherically bent Ge(733) or Ge(800) crystals. Except for the spectrum in Fig. 1(a), which was measured without the polarization analysis, we used the latter analyzer to keep space in the spectrometer for the polarization-analyzing device. The total energy resolution estimated from the full width at half maximum (FWHM) of the elastic peak was about 400 and 600 meV for the Ge(733) and Ge(800) crystals, respectively. For the polarization analysis of the scattered x-rays, a pyrolytic graphite (PG) crystal was placed in front of the detector and the (006) reflection of PG was measured. The scattering angle (θ_P) of the reflection at 8994 eV is 38° and the polarization extinction ratio ($\sin^2 2\theta_P$) is 0.94. Experimental reflectivity of the (006) reflection was about 0.02. By rotating the PG crystal and the detector about the axis of the beam, one can select the polarization of the scattered photon.

A single crystal of $KCuF_3$ was used. Polytype structures corresponding to different stacking of the *ab* plane have been reported to exist in $KCuF_3$.[20] Our single crystal was carefully prepared so that it only contains the (a)-type structure. This was confirmed by a magnetic susceptibility measurement where we observed a single antiferromagnetic transition at 38 K.[21] We use the Miller indices in the tetragonal unit cell of the primitive perovskite structure ($a = 4.1410$ Å and $c = 3.9237$ Å) to represent the momentum transfer ($\boldsymbol{Q}$). The propagation vector of the orbital order is (1/2,1/2,1/2). All the spectra were measured at room temperature.

A typical RIXS spectrum of $KCuF_3$ is shown in Fig. 1(a). The 1.2 eV peak corresponds to orbital excitations which are the subject of this letter. The incident photon energy is fixed at 8994 eV, near the peak of the x-ray absorption spectrum of polycrystalline $KCuF_3$, as shown in Fig. 1(b), where the intensity of the 1.2 eV excitation is maximum. Detailed incident energy dependence and assignment of the excitations at higher energy will be published elsewhere.

The polarization-analyzed RIXS spectra of the 1.2 eV feature are presented in Fig. 2 for four different crystal orientations schematized in the corresponding insets. The incident photon polarization ($\boldsymbol{\epsilon}_i$) lies in the scattering plane and

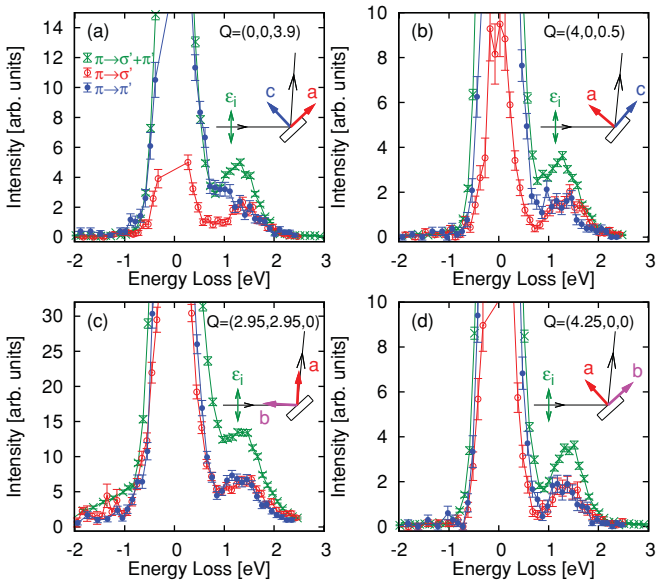

FIG. 2. (Color online) Polarization-analyzed RIXS spectra. Spectra with filled and open circles are measured in the $\pi \rightarrow \sigma'$ and $\pi \rightarrow \pi'$ conditions, respectively. The spectra without polarization analysis are also shown (crosses). Corresponding experimental geometries are shown in insets.

the scattering angle (2θ) is chosen to be close to 90° in order to reduce the elastic scattering. The incident and scattered polarizations are therefore orthogonal to each other, which is the so-called depolarized configuration. In each plot, the spectra are normalized as follows. We first estimated the elastic contribution by fitting of the anti-Stokes region and subtracted it from the raw data. Then the normalization factor, which corresponds to the reflectivity of the polarization-analyzer crystal, was determined so that the sum of the intensity of the $\pi \rightarrow \sigma'$ and $\pi \rightarrow \pi'$ inelastic signals is equal to the $\pi \rightarrow \sigma' + \pi'$ one. Here π is the incident photon polarization parallel to the scattering plane while π' and σ' denote the scattered photon polarizations parallel and perpendicular to the scattering plane, respectively. The polarization conditions corresponding to the different geometrical configurations in Fig. 2 are summarized in Table I. The unit lattice vectors of the crystal are noted as $\boldsymbol{a}$, $\boldsymbol{b}$, and $\boldsymbol{c}$. The unit vectors $\boldsymbol{x}$, $\boldsymbol{y}$, and $\boldsymbol{z}$ are taken so that the hole orbital is represented as $x^2 - y^2$. It is noted that there are two polarization conditions in the xyz coordinates because of the two orbital sublattices, as illustrated in the inset of Fig. 1.

The most striking observation of this measurement is that the spectra show a clear dependence on the scattered photon polarization, that is, additional intensity is found around 1 eV in the spectrum of $\pi \rightarrow \pi'$ compared with $\pi \rightarrow \sigma'$ in the configurations of (a) and (b), whereas the spectra in (c) and (d) are almost identical between the two polarization conditions. In order to identify the observed excitations, we treat theoretically the polarization dependence of RIXS from a phenomenological viewpoint, without identifying the microscopic scattering processes. The scattering cross section in RIXS is represented by the correlation function of the polarizability operator, corresponding to the S matrix, as a function of momentum and the photon polarizations.[22,23]

TABLE I. Summary of the polarization conditions of Fig. 2.

Configuration	Polarization	$\boldsymbol{\epsilon}_i$	$\boldsymbol{\epsilon}_f$	Symmetry of $P_i \times P_f$
(a)	$\pi \rightarrow \sigma'$	$y+z$	x	$A_{2g}+B_{2g}+E_g$
	$(a+c) \rightarrow b$	$x+y$	z	E_g
	$\pi \rightarrow \pi'$	$y+z$	$y-z$	$A_{1g}+B_{1g}+E_g$
	$(a+c) \rightarrow (a-c)$	$x+y$	$x-y$	$B_{1g}+A_{2g}$
(b)	$\pi \rightarrow \sigma'$	$y+z$	x	$A_{2g}+B_{2g}+E_g$
	$(a+c) \rightarrow b$	$x+y$	z	E_g
	$\pi \rightarrow \pi'$	$y+z$	$y-z$	$A_{1g}+B_{1g}+E_g$
	$(a+c) \rightarrow (a-c)$	$x+y$	$x-y$	$B_{1g}+A_{2g}$
(c)	$\pi \rightarrow \sigma'$	z	y	E_g
	$a \rightarrow c$	y	x	$A_{2g}+B_{2g}$
	$\pi \rightarrow \pi'$	z	x	E_g
	$a \rightarrow b$	y	z	E_g
(d)	$\pi \rightarrow \sigma'$	$x+z$	y	$A_{2g}+B_{2g}+E_g$
	$(a+b) \rightarrow c$	$y+z$	x	$A_{2g}+B_{2g}+E_g$
	$\pi \rightarrow \pi'$	$x+z$	$x-z$	$A_{1g}+B_{1g}+E_g$
	$(a+b) \rightarrow (a-b)$	$y+z$	$y-z$	$A_{1g}+B_{1g}+E_g$

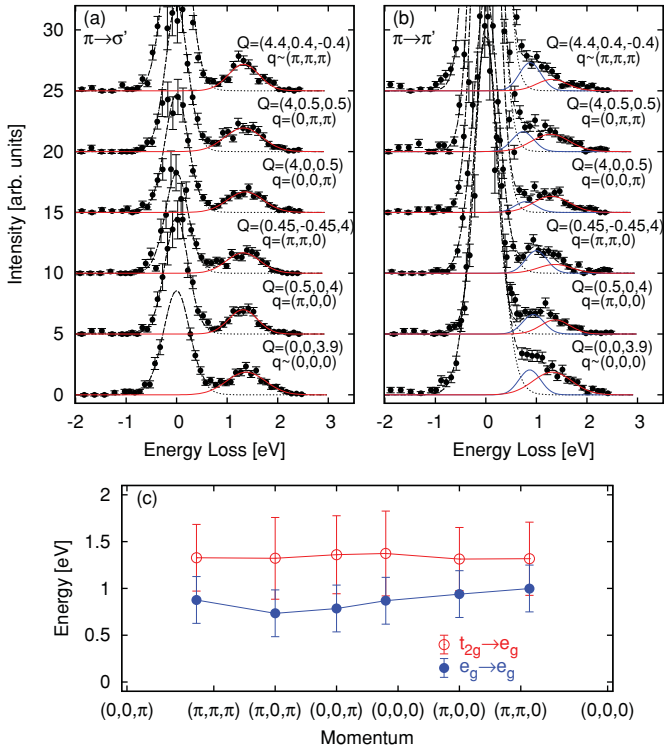

FIG. 3. (Color online) (a) and (b) Momentum dependence of polarization-analyzed RIXS spectra. $\boldsymbol{Q}$ and $\boldsymbol{q}$ are the absolute and reduced momentum transfer, respectively. The filled circles correspond to the experimental data and solid-line spectra are the fitted orbital excitations. Dashed-line spectra represent the sum of the fitted elastic line (dotted line) with the fitted orbital excitations (solid line). (c) Dispersion relation of the orbital excitations. The peak positions are indicated by the circles and the bars denote the FWHM of the excitations.

This operator is expanded in terms of the excitation modes based on the group theoretical analyses. When the electronic excitations occur at the local site where the x-ray is absorbed, there is a selection rule for RIXS that at least one common symmetry should be shared in reduced product-representations $\Gamma_i \times \Gamma_f$ and $P_i \times P_f$. Here $\Gamma_{i(f)}$ and $P_{i(f)}$ are the irreducible representations for the initial (final) electronic orbital and those of the incident (scattered) photon polarization, respectively. Equivalently, the excitations are allowed only if the product-representation $P_i \times P_f \times \Gamma_i$ contains the final state symmetry Γ_f. When other sites are involved in the electronic excitations, this selection rule is modified and depends on the momentum transfer $\mathbf{Q}$.

We approximately treat the local symmetry of the Cu atom as D_{4h} instead of the exact site symmetry of D_{2h} because the Cu-F distances along the x and y directions are almost equal. If only considering onsite excitations, the possible excitation modes in each polarization configuration of the measurements are given by $P_i \times P_f$. Those are listed in Table I. The symmetry of $P_i \times P_f$ has to be either A_{2g} ($\Gamma_{xy} \times \Gamma_{x^2-y^2}$) or E_g ($\Gamma_{yz}, \Gamma_{zx} \times \Gamma_{x^2-y^2}$) for the observation of the t_{2g} excitation and either symmetry is always present in all four experimental configurations of Fig. 2. Accordingly, the t_{2g} excitations are ascribed to the spectral weight observed around 1.3 eV for all configurations and polarization conditions. It is seen to form a peak-like feature except for the $\pi \rightarrow \pi'$ spectra in Figs. 2(a) and 2(b), where it is enmeshed in the high-energy tail of the RIXS spectral weight. On the other hand, e_g excitation requires B_{1g} ($\Gamma_{3z^2-r^2} \times \Gamma_{x^2-y^2}$) polarization symmetry, which exists in the $\pi \rightarrow \pi'$ condition for the configurations of Figs. 2(a), 2(b), and 2(d). Assuming that the symmetry argument gives a necessary condition for the observation by RIXS, the additional intensity observed around 1 eV in the $\pi \rightarrow \pi'$ polarization of the Figs. 2(a) and 2(b) is ascribed to the e_g excitation. We briefly comment on the absence of e_g excitation in the spectrum obtained in the $\pi \rightarrow \pi'$ condition of the configuration for Fig. 2(d). From our symmetry analysis, the weight of the B_{1g} component for the $\pi \rightarrow \pi'$ polarization in the configuration of Fig. 2(d) is deduced to be 40% of that for the $\pi \rightarrow \pi'$ polarization of Figs. 2(a) and 2(b). For a quantitative agreement with the experiment, one may need to carry out a theoretical evaluation of the intensity including a microscopic description of the RIXS process.

Our assignments based on the polarization analysis are consistent with a recent optical absorption study,[24,25] where the different orbital excitations were identified and their respective energies estimated. The e_g excitation is located at 1.02 eV in the optical absorption spectrum while the t_{2g} excitations are at 1.15, 1.37, and 1.46 eV, respectively. These t_{2g} excitations are found to appear as a single peak in the RIXS spectrum within our resolution.

Now that we are able to distinguish the e_g excitation from the t_{2g} excitations, it becomes possible to investigate the momentum dependence of each kind of orbital excitations separately. Figures 3(a) and 3(b) show the polarization-analyzed RIXS spectra obtained near the high-symmetry points of the Brillouin zone. Here $\boldsymbol{q}$ is the momentum transfer in the reduced Brillouin zone. The spectra of the upper and lower three momenta in each figure are measured at or near the

configurations of Figs. 2(a) and 2(b), respectively. In order to elucidate the dispersion relation of the orbital excitations quantitatively, we fit the whole set of RIXS spectra in Figs. 3(a) and 3(b). We start with the spectra collected with the $\pi \rightarrow \sigma'$ polarization in Fig. 3(a), where only the t_{2g} excitations are observed. The tail of the elastic scattering or quasielastic component on the energy loss side was evaluated from the energy-gain side. The excitation peak was approximated by a single Gaussian function. We then fit the spectra obtained in the $\pi \rightarrow \pi'$ condition in Fig. 3(b), using the positions and widths of the t_{2g}-excitation peak inferred from the fits of the spectra in Fig. 3(a) and keeping them fixed. The peak centers and FWHMs used in the fits are plotted as functions of the reduced momentum transfer in Fig. 3(c). The dispersion relation of the excitations is found to be small for both excitations. It is noteworthy that the dispersion of the excitation between the two e_g orbitals, which corresponds to the orbital order in $KCuF_3$, is not discernible within the experimental resolution. This result suggests that the Jahn-Teller splitting between the two e_g orbitals is about 1 eV irrespective of the momentum transfer. Moreover, we conclude that the intersite interactions between the d orbitals, which can be ascribed to the magnitude of the dispersion, are much smaller in energy than the experimental resolution (600 meV). Overall, these data importantly show that RIXS at the K edge can be used as a robust technique that provides information about the dependence of the electronic excitations upon two key parameters of the condensed matter physics, momentum, and polarization. Since improvement of the energy resolution is still in progress; the dispersion relation of orbital excitations should become observable by K-edge RIXS in the near future.

In summary, we have performed a polarization-analyzed resonant inelastic x-ray scattering study of the orbital excitations in $KCuF_3$ at the Cu K edge. The polarization of the scattered photons in RIXS was identified for the first time. A clear polarization dependence is observed in the inelastic spectrum, which we interpreted via a phenomenological consideration of the RIXS process that provides us with a necessary condition for the appearance of the orbital excitations. Doing so, we could distinctly identify the excitation between the e_g orbitals and the excitations from the t_{2g} orbitals to the e_g orbital. Taking advantage of our polarization analysis, we were able to successfully measure the momentum dependence of the excitation corresponding to the orbital degree of freedom over the whole Brillouin zone and found that the excitation is nearly dispersionless within our experimental resolution.

This work was performed under the interuniversity cooperative research program of the Institute of Materials Research, Tohoku University, and financially supported by the Grant-in-Aid for Young Scientists (B) (No. 20740179) from JSPS.

[1] S. Maekawa *et al.*, *Physics of Transition Metal Oxides* (Springer, 2004).
[2] E. Saitoh *et al.*, Nature (London) **410**, 180 (2001).
[3] B. C. Larson, J. Z. Tischler, W. Ku, C. C. Lee, O. D. Restrepo, A. G. Eguiluz, P. Zschack, and K. D. Finkelstein, Phys. Rev. Lett. **99**, 026401 (2007).
[4] A. Kotani *et al.*, Rev. Mod. Phys. **73**, 203 (2001).
[5] M. Z. Hasan *et al.*, Science **288**, 1811 (2000).
[6] K. Ishii *et al.*, Phys. Rev. Lett. **94**, 207003 (2005).
[7] J. Kim, D. S. Ellis, H. Zhang, Y. J. Kim, J. P. Hill, F. C. Chou, T. Gog, and D. Casa, Phys. Rev. B **79**, 094525 (2009).
[8] J. P. Hill *et al.*, Phys. Rev. Lett. **100**, 097001 (2008).
[9] L. Braicovich *et al.*, Phys. Rev. Lett. **102**, 167401 (2009).
[10] J. Schlappa *et al.*, Phys. Rev. Lett. **103**, 047401 (2009).
[11] Y.-J. Kim, J. P. Hill, F. C. Chou, D. Casa, T. Gog, and C. T. Venkataraman, Phys. Rev. B **69**, 155105 (2004).
[12] C. Ulrich *et al.*, Phys. Rev. Lett. **103**, 107205 (2009).
[13] K. Hämäläinen, J. P. Hill, S. Huotari, C. C. Kao, L. E. Berman, A. Kotani, T. Ide, J. L. Peng, and R. L. Greene, Phys. Rev. B **61**, 1836 (2000).
[14] T. Idé *et al.*, J. Phys. Soc. Jpn. **69**, 3107 (2000).
[15] L. Lu, J. N. Hancock, G. Chabot-Couture, K. Ishii, O. P. Vajk, G. Yu, J. Mizuki, D. Casa, T. Gog, and M. Greven, Phys. Rev. B **74**, 224509 (2006).
[16] M. Takahashi *et al.*, J. Phys. Soc. Jpn. **77**, 034711 (2008).
[17] F. Vernay, B. Moritz, I. S. Elfimov, J. Geck, D. Hawthorn, T. P. Devereaux, and G. A. Sawatzky, Phys. Rev. B **77**, 104519 (2008).
[18] P. Abbamonte *et al.*, e-print arXiv:cond-mat/9911215.
[19] K. Hirakawa *et al.*, J. Phys. Soc. Jpn. **23**, 756 (1967).
[20] A. Okazaki, J. Phys. Soc. Jpn. **26**, 870 (1969).
[21] M. T. Hutchings *et al.*, Phys. Rev. **188**, 919 (1969).
[22] S. Ishihara and S. Maekawa, Phys. Rev. B **62**, R9252 (2000).
[23] S. Ishihara *et al.*, Physica B **345**, 15 (2004).
[24] J. Deisenhofer, I. Leonov, M. V. Eremin, C. Kant, P. Ghigna, F. Mayr, V. V. Iglamov, V. I Anisimov, and D. vanderMarel, Phys. Rev. Lett. **101**, 157406 (2008).
[25] In general, electric dipole transitions between d orbitals are parity forbidden, but they can become allowed by assistance of phonons.